

# Small-Angle Neutron Scattering Study of Poly(vinyl alcohol) Gels During Melting Process

Nobuaki Takahashi, Toshiji Kanaya, Koji Nishida, Keisuke Kaji

*Institute for Chemical Research, Kyoto University, Uji, Kyoto-fu 611-0011, Japan*

Received 16 October 2003; accepted 14 April 2004

DOI 10.1002/app.20818

Published online in Wiley InterScience (www.interscience.wiley.com).

**ABSTRACT:** Small-angle neutron scattering (SANS) measurements were performed on poly(vinyl alcohol) (PVA) gels in a mixture of deuterated dimethyl sulfoxide (DMSO- $d_6$ ) and  $D_2O$  with volume ratio of 60/40 to see the structure changes of the crosslinking points, which are crystallites, and of the gel network during the melting process. The observed SANS intensities were fitted to the Ornstein-Zernike (OZ) formula and a power law in scattering vector  $Q$  ranges from 0.01 to 0.035 and 0.05 to 0.1  $\text{\AA}^{-1}$ , respectively, to evaluate the correlation length  $\xi$  and the power law exponent  $n$ . It was found that the exponent  $n$  is 4 and the correlation length  $\xi$  is  $\sim 150$   $\text{\AA}$  below  $\approx 70^\circ\text{C}$ , suggesting that the crystallite surface is smooth and the average distance

between the neighboring crystallites is  $\approx 150$   $\text{\AA}$ . On the other hand, they begin to decrease  $>70^\circ\text{C}$ . The decrease of  $n$  suggests that the surface of the crystallites becomes rougher with increasing temperature. As for the correlation length  $\xi$ , analyses in terms of distance distribution function suggested that the decrease of  $\xi$  is apparent, and the intercrystallite distance increases with temperature  $>70^\circ\text{C}$  because the crystallites decrease in number because of melt. © 2004 Wiley Periodicals, Inc. *J Appl Polym Sci* 95: 157–160, 2005

**Key words:** poly(vinyl alcohol); gel; melting process; small-angle neutron scattering; distance distribution function

## INTRODUCTION

Polymer gels were extensively studied from various points of view<sup>1–5</sup> because they have many interesting features such as high solvent absorptive power, soft elasticity, responsibility for electric field, pH, and magnetic field. Poly(vinyl alcohol) (PVA) is one of the most interesting gel-forming polymers because it is water soluble and biocompatible. PVA gels formed in mixtures of dimethyl sulfoxide (DMSO) and water also show very interesting features, depending on the mixing ratio (e.g., gels formed in a mixture of DMSO/water = 60/40 below  $-20^\circ\text{C}$  are transparent, the elasticity is very high, and the gelation rate is very fast compared with those from aqueous solutions). We therefore studied the formation process, structure, and stability of PVA gels in a mixture of DMSO and water with volume ratio of 60/40.<sup>6–13</sup> In these studies, it was revealed by small-angle neutron scattering (SANS) and wide-angle neutron scattering (WANS) techniques<sup>8</sup> that the crosslinking points are small crystallites with a size of  $\sim 70$   $\text{\AA}$  and the distance of the nearest neighboring crystallites are  $\sim 180$   $\text{\AA}$ ; the structure strongly affects many properties of the gels such as elasticity and solvent absorptive power. In the case of the PVA gels, it is expected that the nature of the

crosslinking points and their distribution depend on temperature because they are crystallites. In this work, therefore, we studied the structure changes of the crystallites and the network of the PVA gel upon heating below and above the melting temperature by using a SANS technique.

## EXPERIMENTAL

Fully saponified atactic PVA with a number-average degree of polymerization  $P = 1730$  was used in this work. The molecular weight distribution  $M_w/M_n$  is 1.97, where  $M_w$  and  $M_n$  are weight- and number-average molecular weights, respectively. The details of the characterization of this sample were reported in the previous article.<sup>6</sup> The solvent used for the experiments was a mixture of deuterated dimethyl sulfoxide (DMSO- $d_6$ ) and heavy water ( $D_2O$ ) with a volume fraction of DMSO- $d_6$   $\phi_{\text{DMSO}} = 0.60$ . PVA concentration  $C_p$  was 5 g/dl.

Gel samples were prepared as follows. A given amount of PVA was dissolved in a solvent at  $\sim 130^\circ\text{C}$  in an autoclave to be homogenized in a glass vial. Before the measurements, the sample in the glass vial was again homogenized at  $100^\circ\text{C}$  for about 30 min, quenched to  $27^\circ\text{C}$ , quickly transferred to the cell, and then left to stand for 24 h to be gelled.

SANS measurements were carried out at 27, 45, 60, 70, 80, 90, and  $100^\circ\text{C}$  on a SANS-U spectrometer<sup>14</sup> at the Neutron Scattering Laboratory of the ISSP (Uni-

Correspondence to: T. Kanaya (Kanaya@scl.kyoto-u.ac.jp).

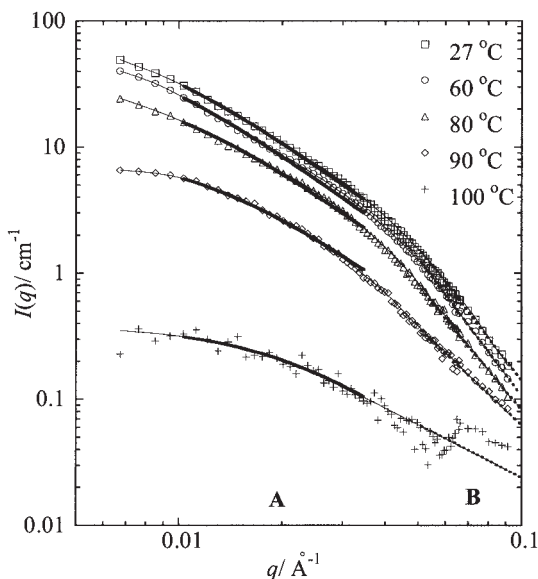


**Figure 1** Small-angle neutron scattering (SANS) intensity  $I(Q)$  from the gel formed at 27°C as a function of temperature  $T$  in double logarithmic form. ( $\square$ ):  $T = 27^\circ\text{C}$ , ( $\circ$ ):  $T = 60^\circ\text{C}$ , ( $\triangle$ ):  $T = 80^\circ\text{C}$ , ( $\diamond$ ):  $T = 90^\circ\text{C}$ , (+):  $T = 100^\circ\text{C}$ . The ranges A and B indicate the  $Q$  ranges between 0.01 and 0.035  $\text{\AA}^{-1}$  and between 0.05 and 0.1  $\text{\AA}^{-1}$ , respectively. The bold and dotted lines indicate the OZ formula and power law, respectively. The thin solid lines are the results of fits to  $I(Q)$  in whole  $Q$  range.

versity of Tokyo, Tokai, Japan). The incident neutron wavelength  $\lambda$  and the dispersion  $\Delta\lambda/\lambda$  were 7  $\text{\AA}$  and 10%, respectively. The scattering neutrons were measured by using a two-dimensional position-sensitive detector of  $65 \times 65 \text{ cm}^2$  ( $128 \times 128$  pixels) area. In the measurements, the scattering vector  $Q (=4\pi\sin\theta/\lambda$ ;  $\lambda$  and  $2\theta$  being neutron wavelength and scattering angle, respectively) ranges from  $5.8 \times 10^{-3}$  to  $9.1 \times 10^{-2}$   $\text{\AA}^{-1}$ .

## RESULTS AND DISCUSSION

Figure 1 shows SANS intensities  $I(Q)$ 's of the PVA gel at 27, 60, 80, 90, and 100°C during the melting process as a function of  $Q$  in double-logarithmic form. Macroscopic change from gel to sol state occurs at about 85°C. This means that  $I(Q)$ 's in the temperature range  $<80^\circ\text{C}$  are from gel and  $I(Q)$ 's  $>90^\circ\text{C}$  are from sol. In the gel state, the scattering intensity  $I(Q)$  decreases gradually with increasing temperature, and it begins to decrease drastically above 80°C. Before going into a detailed discussion, we recall the results of the previous studies,<sup>8,9</sup> which gave us the basis of interpretation of this experiment.

We studied the structure of the PVA gel at 23°C by using SANS and WANS techniques.<sup>8,9</sup> In the WANS measurements, the Bragg peaks from (101) and (10 $\bar{1}$ ) planes of PVA crystallites<sup>15</sup> were clearly observed,

showing that the crystallites exist in the gels. Furthermore, as temperature increases, the peaks disappear at  $\sim 85^\circ\text{C}$ , corresponding to the macroscopic melting of the gel. From these observations, we could directly conclude that the crosslinking points are crystallites. In the SANS measurements, it was found that the intensity  $I(Q)$  from the gel is well described by the Ornstein-Zernike (OZ) formula [eq. (1)] and the Porod's law [eq. (2)] in  $Q$ -ranges from 0.01 to 0.035  $\text{\AA}^{-1}$  and from 0.05 to 0.1  $\text{\AA}^{-1}$ , respectively,

$$I(Q) = \frac{I(0)}{1 + \xi^2 Q^2} \quad (0.01 \text{ \AA}^{-1} < Q < 0.035 \text{ \AA}^{-1}) \quad (1)$$

$$I(Q) \sim Q^{-4} \quad (0.05 \text{ \AA}^{-1} < Q < 0.1 \text{ \AA}^{-1}) \quad (2)$$

where  $\xi$  is a correlation length and  $I(0)$  is a scattering intensity at  $Q = 0$ . As mentioned above, the crosslinking points are crystallites, and hence, the correlation length  $\xi$  was assigned to the average distance between nearest neighboring crystallites.<sup>8</sup>

The Porod's law observed here suggests that the surfaces of the crystallites are very smooth. According to the concept of surface fractal,<sup>16</sup> scattering intensity  $I(Q)$  obeys a power law formula  $I(Q) \approx Q^{-n}$ , where the exponent  $n$  is related to the surface fractal dimension  $d_s$  through  $n = 2d - d_s$  in  $d$ -dimensional space. In three-dimensional space, for example, the range of  $d_s$  is from 2 to 3, corresponding to the range of  $n$  from 4 to 3. The Porod's law  $I(Q) \approx Q^{-4}$  is a particular case of surface fractal scattering.

Following the previous analysis, we fitted the OZ formula and the power law to the observed intensity in  $Q$ -ranges between 0.01 and 0.035  $\text{\AA}^{-1}$  and between 0.05 and 0.1  $\text{\AA}^{-1}$ , respectively, which are indicated by A and B in Figure 1. Bold lines and dotted lines in the figure are the results of fits with the OZ formula and the power law, respectively. The evaluated correlation length  $\xi$  and the exponent  $n$  from the fits are plotted against temperature in Figure 2.

The exponent  $n$  is  $\sim 4$  at 27°C and is almost independent of temperature up to 70°C, showing that the boundary of the crystallites is smooth and independent of temperature  $<70^\circ\text{C}$ . On the other hand, it begins to decrease above 70°C. At 80°C below the melting temperature, the value of  $n$  is 3.4. According to the concept of surface fractal, this means that the crystalline surfaces do not maintain clear boundaries but become rougher with increasing temperature. At 90°C above the melting temperature, the value of  $n$  is 2.5, which is  $<3$ . If we observe the surface scattering, the range of  $n$  should be between 4 and 3, corresponding to change from two to three dimensions. Therefore, we cannot apply the surface fractal concept to the data  $>90^\circ\text{C}$ . This means that there are no boundaries of crystallites because of melt.

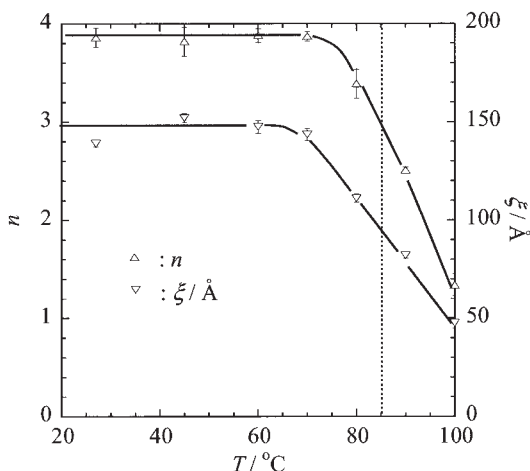


**Figure 2** Temperature dependence of the exponent  $n$  and correlation length  $\xi$ . The dotted vertical line, indicating  $T = 85^\circ\text{C}$ , is the macroscopic gel melting temperature.

The correlation length  $\xi$  is also independent of temperature  $<70^\circ\text{C}$ , as seen in Figure 2. This indicates that the average distance between the nearest neighboring crystallites does not change  $<70^\circ\text{C}$ . In other words, the network structure hardly changes up to  $70^\circ\text{C}$ . On the other hand, the scattering intensity decreases with increasing temperature even  $<70^\circ\text{C}$ . This can be understood in terms of the temperature factor or the Debye–Waller factor. In the measurements, we are mainly seeing the intercrystallite correlations. The scattering intensity from the correlations is weakened because of the thermal fluctuations of the crystallites. In our previous neutron spin-echo measurements,<sup>13</sup> the root-mean-square displacement of the crystallite due to the fluctuations  $\sqrt{\langle u^2 \rangle}$  was estimated to be 8.2 Å around its quasi-equilibrium position at  $25^\circ\text{C}$ . As temperature increases, the fluctuations must be enhanced, leading to a larger Debye–Waller factor, and hence, the scattering intensity decreases.

Above  $70^\circ\text{C}$ , the correlation length  $\xi$  begins to decrease with increasing temperature even below the melting temperature (see Fig. 2). This result is contrary to our expectations. As temperature increases near the melting temperature, the smaller crystallites would melt at lower temperatures than the melting temperature of the gel ( $=85^\circ\text{C}$ ), and it is expected that the correlation length  $\xi$  or the average distance between the nearest neighboring crystallites must increase because the number of crystallites decreases even below the melting temperature. Above the melting temperature of the gel, most crystallites melt or even if some large crystallites survive the number of crystallites are very little, and hence, the correlation length must increase. However, the correlation length  $\xi$  decreases with increasing temperature  $>70^\circ\text{C}$  (see Fig. 2). How can we understand this result?

To attack this problem, we have calculated the distance distribution function  $P(r)$ , which is defined by

inverse Fourier transformation of scattering intensity  $I(Q)$ ,<sup>17</sup>

$$P(r) \sim \frac{2}{\pi} \int r Q I(Q) \sin(rQ) dQ \sim 4\pi r^2 \gamma(r) \quad (3)$$

where  $\gamma(r)$  is a pair correlation function. For calculation of eq. (3), we have to extrapolate the observed scattering curves to both the lower and the higher  $Q$  ranges. This was made by employing the OZ formula and the power law for the lower and higher  $Q$  ranges, respectively. This procedure did neglect deviation of  $I(Q)$  from the OZ formula in the  $Q$  range  $<0.01 \text{ \AA}^{-1}$ , meaning that we have to eliminate the larger structure in  $P(r)$ . The calculated distance distribution functions  $P(r)$  at various temperatures are shown by bold lines in Figure 3. Two broad peaks or shoulders are observed at about 70 and 180 Å in  $P(r) < 70^\circ\text{C}$ . These two peaks or shoulders were assigned to the intra- and intercrystallite correlations, respectively.<sup>8,9</sup> To separate the two contributions, we fitted the observed  $P(r)$

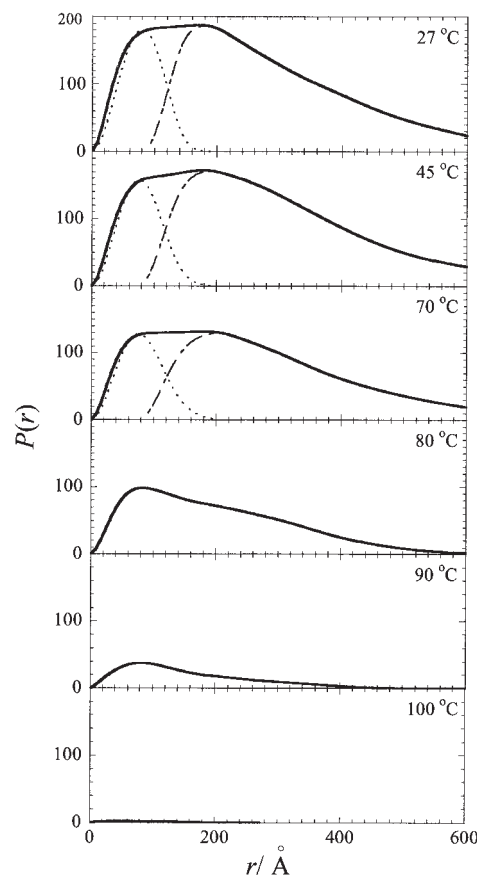


**Figure 3** Distance distribution function  $P(r)$  obtained by inverse Fourier transformation of  $I(Q)$  as a function of temperature (bold lines). Dotted and dashed lines indicate the distance distribution function due to the intracrystallite correlation  $P_{\text{intra}}(r)$  and due to the intercrystallite correlation  $P_{\text{inter}}(r)$ , respectively.

in the small  $r$  range with a model function  $P_{\text{intra}}(r)$  for the intracrystallite correlation. This model function was calculated under an assumption that the shape of the crystallites is a sphere and the size (radius) distribution of the crystallites can be represented by a Gaussian. The intercrystallite correlation  $P_{\text{inter}}(r)$  was obtained by subtracting  $P_{\text{intra}}(r)$  from the total  $P(r)$ . The resultant  $P_{\text{intra}}(r)$  and  $P_{\text{inter}}(r)$  are shown by dotted and dashed lines in Figure 3, respectively. Both peak positions of  $P_{\text{intra}}(r)$  and  $P_{\text{inter}}(r)$  hardly move upon heating  $<70^\circ\text{C}$ , whereas the peak intensities of  $P_{\text{intra}}(r)$  and  $P_{\text{inter}}(r)$  decrease. These results correspond to the facts that the  $\xi$  is independent of temperature and the SANS intensity decreases with temperature, respectively. At  $80^\circ\text{C}$ , the shoulder cannot be recognized at  $\sim 200 \text{ \AA}$  but at  $300 \text{ \AA}$ , the intensity becomes weak. This suggests that the number of crystallites decreases and the average distance between the nearest neighboring crystallites increases. At  $90^\circ\text{C}$  above the melting temperature of the gel, the intercrystallites correlation disappears and only a broad peak is observed at  $\sim 70 \text{ \AA}$ . This peak must be due to intracrystallite correlation surviving even above the melting temperature of the gel or concentration fluctuations at the positions where crystallites were. In any case, there are few crystallites or only concentration fluctuations in the system. Finally, at  $100^\circ\text{C}$ , the correlation peak almost disappears, meaning that the gel completely melts. In the evaluation of  $\xi$  from the OZ fit to the scattering intensity (see Fig. 1), the contribution of the intercrystallite contribution is so small that the value of  $\xi$  is dominated by the intracrystallite correlation, leading to apparently small  $\xi$ . This is the reason the correlation length decreases with increasing temperature. Therefore, the correlation length  $\xi$  at  $80^\circ\text{C}$  should not be considered as the average distance between the nearest neighboring crystallites.

### CONCLUSION

The structural change during the melting process of PVA gel was investigated by using SANS. The observed scattering intensities were fitted to the OZ formula and the power law in  $Q$  ranges of 0.01 to 0.035

$\text{\AA}^{-1}$  and 0.05 to  $0.1 \text{ \AA}^{-1}$ , respectively, to evaluate the correlation length  $\xi$  and the power law exponent  $n$ . On the basis of the temperature dependence of  $\xi$  and  $n$ , it was revealed that the change of the gel structure upon heating begins at  $\sim 70$  or  $15^\circ\text{C}$  below the macroscopic melting temperature of the gel ( $=85^\circ\text{C}$ ). Below the melting temperature, the smooth surface of the crystallite becomes rougher and the crystallites decrease in number with increasing temperature. The analyses in terms of distance distribution function also suggested that there are surviving crystallites or large concentration fluctuations even at  $90^\circ\text{C}$  above the melting temperature, meaning that the sol is not a homogeneous solution at  $90^\circ\text{C}$ . At  $100^\circ\text{C}$ , they completely disappear and only solution-like concentration fluctuations remain. Thus, this study revealed microscopic structure changes of the PVA gel during the melting process.

### References

1. de Gennes, P. G. *Scaling Concepts in Polymer Physics*; Cornell University Press; Ithaca, 1979.
2. Kramer, O. *Biological and Synthetic Polymer Networks*; Elsevier Applied Science; London, 1988.
3. Buchard, W.; Ross-Murphy, S. B. *Physical Networks: Polymers and Gels*; Elsevier Applied Science; London, 1990.
4. Guenet, J. *Thermoreversible Gelation of Polymers and Biopolymers*; Academic Press; London, 1992.
5. Aharoni, S. M. *Synthesis, Characterization, and Theory of Polymeric Networks and Gels*; Plenum: New York, 1992.
6. Ohkura, M.; Kanaya, T.; Kaji, K. *Polymer* 1992, 33, 3689.
7. Ohkura, M.; Kanaya, T.; Kaji, K. *Polymer*, 1992, 33, 5044.
8. Kanaya, T.; Ohkura, M.; Kaji, K.; Furusaka, M.; Misawa, M. *Macromolecules* 1994, 27, 5609.
9. Kanaya, T.; Ohkura, M.; Takeshita, H.; Kaji, K.; Furusaka, M.; Yamaoka, H.; Wignall, G. D. *Macromolecules* 1995, 28, 3168.
10. Kanaya, T.; Takeshita, H.; Nishikoji, Y.; Ohkura, M.; Nishida, K.; Kaji, K. *Supramol Sci* 1998, 5, 215.
11. Takeshita, H.; Kanaya, T.; Nishida, K.; Kaji, K. *Macromolecules* 1999, 32, 7815.
12. Takeshita, H.; Kanaya, T.; Nishida, K.; Kaji, K.; Hashimoto, M.; Takahashi, T. *Phys Rev E* 2000, 61, 2125.
13. Kanaya, T.; Takahashi, N.; Nishida, K.; Kaji, K.; Seto, H.; Nagao, M.; Kawabata, Y.; Takeda, T., *J Neutron Res* 2002, 14, 10, 149.
14. Ito, Y.; Imai, M.; Takahashi, S. *Physica B* 1995, 213/214, 889.
15. Bunn, C. W. *Nature* 1948, 161, 929.
16. Martin, J. E.; Hurd, A. J. *J Appl Crystallogr* 1987, 20, 61.
17. Kaji, K.; Urakawa, H.; Kanaya, T.; Kitamaru, R. *Macromolecules* 1984, 17, 1835.